Pharmacological Research 70 (2013) 90–101

Contents lists available at SciVerse ScienceDirect

Pharmacological Research

journal homepage: www.elsevier.com/locate/yphrs

PIM1 kinase inhibitors induce radiosensitization in non-small cell lung cancer cells

Wanyeon Kim[a], HyeSook Youn[b], TaeWoo Kwon[a], JiHoon Kang[a], EunGi Kim[a], Beomseok Son[a], Hee Jung Yang[a], Youngmi Jung[a], BuHyun Youn[a,*]

[a] Department of Biological Sciences, Pusan National University, Busandaehak-ro 63, Geumjeong-gu, Busan, 609-735, South Korea
[b] Department of Bioscience & Biotechnology/Institute of Bioscience, Sejong University, 98 Gunja-dong, Gwangjin-gu, Seoul, 143-747, South Korea

ARTICLE INFO

Article history:
Received 7 November 2012
Received in revised form 7 January 2013
Accepted 14 January 2013

Keywords:
Radiosensitizer
PIM1 inhibitor
SGI-1776
ETP-45299
Tryptanthrin
Non-small cell lung cancer

ABSTRACT

Radiotherapy plays a critical role in the treatment of non-small cell lung cancer (NSCLC). However, radioresistance is a major barrier against increasing the efficiency of radiotherapy for NSCLC. To understand the mechanisms underlying NSCLC radioresistance, we previously focused on the potential involvement of PIM1, PRAS40, FOXO3a, 14-3-3, and protein phosphatases. Among these proteins, PIM1 functioned as an oncogene and was found to act as a crucial mediator in radioresistant NSCLC cells. Therefore, we investigated the use of PIM1-specific inhibitors as novel therapeutic drugs to regulate radiosensitivity in NSCLC. After structure-based drug selection, SGI-1776, ETP-45299, and tryptanthrin were selected as candidates of PIM1 inhibitors that act as radiosensitizers. With irradiation, these drugs inhibited only PIM1 kinase activity without affecting PIM1 mRNA/protein levels or cellular localization. When PIM1 kinase activity was suppressed by these inhibitors, PRAS40 was not phosphorylated. Consequently, unphosphorylated PRAS40 did not form trimeric complexes with 14-3-3 and FOXO3a, leading to increased nuclear localization of FOXO3a. Nuclear FOXO3a promoted the expression of pro-apoptotic proteins such as Bim and FasL, resulting in a radiosensitizing effect on radioresistant NSCLC cells. Moreover, an *in vivo* xenograft mouse model confirmed this radiosensitizing effect induced by PIM1 inhibitors. In these model systems, tumor volume was significantly reduced by a combinational treatment with irradiation and PIM1 inhibitors compared to irradiation alone. Taken together, our findings provided evidence that PIM1-specific inhibitors, SGI-1776, ETP-45299, and tryptanthrin, can act as novel radiosensitizers to enhance the efficacy of radiotherapy by inhibiting irradiation-induced signaling pathway associated with radioresistance.

1. Introduction

Lung cancer is the most frequent cause of cancer death throughout the world. Lung cancer is categorized into small cell lung cancer (SCLC) and non-small cell lung cancer (NSCLC) based on cancer cell histology [1]. Between the two types, NSCLC accounts for about 80–85% of total lung malignancies [2]. Only 15–20% of NSCLC patients diagnosed at early stage could be cured successfully by surgical resection, while over 50% of NSCLC patients were often diagnosed at advanced stages and curative surgical removal could not be performed to their tumors. Therefore, radiotherapy is preferred to an alternative treatment for them [3]. However, recurrence rates and metastasis still remain high and the therapeutic outcome of most NSCLC patients is not satisfactory. The emergence of radioresistance is regarded as one of the major factors for therapy failure. Although enhanced efficacy of radiotherapy could be expected by dose escalation, this protocol might be restricted by considerable cytotoxicity associated with high dose irradiation. Thus, there are many efforts to regulate radioresistance and develop potent radiosensitizers for establishing better treatment strategies. Various experimental and clinical studies suggest that radioresistance is positively associated with the overexpression and activation of specific genes, including ones encoding epidermal growth factor receptor (EGFR), c-Raf, p53 and PIM1 [4–7]. Although such findings have contributed to limited information of the mechanism underlying cellular radioresistance, there are presently no molecular targeted therapies that can be effectively

Abbreviations: ASK1, apoptosis signaling kinase 1; ChIP, chromatin immunoprecipitation; CK2, casein kinase 2; DMSO, dimethyl sulfoxide; FOXO, the mammalian forkhead box transcription factors of the O classification; EGFR, epidermal growth factor receptor; FasL, Fas ligand; FRE, FOXO-response element; HA, Hemagglutinin; HNSCC, head and neck squamous cell carcinoma; IR, ionizing radiation; ITC, isothermal titration calorimetry; NSCLC, non-small cell lung cancer; PRAS40, proline-rich AKT substrate of 40 kDa; SAR, structure–activity relationship; SCLC, small cell lung cancer; SD, standard deviation.

* Corresponding author at: #303 Biology Building, Department of Biological Sciences, Pusan National University, Busandaehak-ro 63, Geumjeong-gu, Busan, 609-735, South Korea. Tel.: +82 51 510 2264; fax: +82 51 581 2962.
E-mail address: bhyoun72@pusan.ac.kr (B. Youn).

1043-6618/$ – see front matter © 2013 Elsevier Ltd. All rights reserved.
http://dx.doi.org/10.1016/j.phrs.2013.01.005

combined with radiation for treating lung cancer. Thus, the identification of biomarker(s) responsible for conferring radioresistance and modification of the irradiation response by radiosensitizers would greatly advance the discovery of drugs that enhance the sensitivity of NSCLC cells to radiation [8–10].

PIM1 is a serine/threonine kinase that acts as a potent mediator of cell survival. PIM1 was originally identified as a proviral integration site in Moloney murine leukemia virus-induced murine T-cell lymphomas. This protein appears to play various biological roles in cell survival, proliferation, and differentiation [11–13]. Although PIM1 alone is weakly oncogenic, it has been demonstrated that PIM1 is closely associated with transformation of malignant cells and acceleration of tumorigenesis [14–18]. Several groups have recently reported the complex crystal structure of PIM1 with nucleotide analogs and a number of small ATP-competitive inhibitors [19–22]. Results of these studies revealed a constitutively active kinase conformation of PIM1 in the absence of phosphorylated residues in the activation loop. In addition, the PIM1 structures have a unique hinge region lacking a hydrogen bond donor, suggesting a possibility for the development of specific PIM1 kinase inhibitors that target the ATP binding site. Based on the characteristic of a constitutively active form, PIM1 activity might rely on the expression level and subcellular localization, like phosphorylase kinase and checkpoint kinase 1 [19,22]. PIM1 kinase plays roles in proliferation and survival for normal physiological and pathological processes through phosphorylation of various cytoplasmic and nuclear proteins. For example, PIM1 can promote cell survival *via* phosphorylation of pro-apoptotic proteins such as Bad and apoptosis signaling kinase 1 (ASK1) [23,24]. Bad phosphorylation on Ser112 by PIM1 exerted an increase of Bcl-2 activity resulting in anti-apoptotic function. PIM1-mediated ASK1 phosphorylation on Ser83 induced ASK1 kinase in an inactive state, leading to inhibition of caspase-3-mediated apoptosis under stress conditions.

In addition to its roles in proliferation and survival, new PIM1 activity has been recently described in our previous study [7]. We demonstrated that IR leads to PIM1 overexpression and a reduction of protein phosphatases (PP2A and PP5), which induces PIM1 translocation into the nucleus in radioresistant NSCLC cells. Increased nuclear PIM1 enhances PRAS40 phosphorylation. Consequently, phosphorylated PRAS40 forms a trimeric complex with 14-3-3 and AKT-activated pFOXO3a, which then moves rapidly into the cytoplasm. Retention of FOXO3a in the cytoplasm is associated with the down-regulation of pro-apoptotic genes and possibly radioresistance. Under these conditions, PIM1-activated pPRAS40, AKT-activated pFOXO3a, and complexes formed by these two proteins and 14-3-3 could be key regulators of IR-induced radioresistance in NSCLC cells. Consistent with our previous data, it has been reported that PIM1 is overexpressed in malignant keratinocytes in head and neck squamous cell carcinoma (HNSCC) and moderate/high PIM1 expression levels tend to be associated with poor prognosis in HNSCC compared to low/negative PIM1 expression [25]. In addition, the expression of PIM1 is also significantly associated with the expression of EGFR, which has been previously demonstrated to promote radioresistance [25,26]. Because the classic prognostic markers such as tumor size, nodal status, or histological grade cannot be used to predict responses to radiotherapy, and there are currently no generally accepted clinical markers for predicting radiosensitivity, these results may have clinical implication. Therefore, it could be concluded that, importantly, PIM1 overexpression significantly correlates with a poor response to radiotherapy.

Due to PIM1 overexpression in various types of tumors as well as the role of this protein in the regulation of pathways considered cancer-related, the development of potent and selective PIM1 inhibitors has a strong therapeutic interest and will provide a powerful tool for dissecting the specific biological functions such as radioresistance. Imidazopyridazine derivatives have been previously described as inhibitors of PIM1 kinase and several groups have reported the complex crystal structure of PIM1 with a number of ATP mimetic kinase inhibitors [19,22,27–29]. Unconventional structural features associated with PIM1 proteins have provided opportunities to identify selective inhibitors without hampering lead finding activities as a number of chemotypes have now been reported as PIM1 kinase inhibitors [30].

Based on our previous data, we hypothesized that PIM1 could be a key regulator of IR-induced radioresistance in NSCLC cells [7]. In order to better understand the biological effects of the pharmacological inhibition of PIM1, we initiated a project to identify potent and selective inhibitors of PIM1 for overcoming the radioresistance of NSCLC cells. In the present study, we report on the ability of two known PIM1 inhibitors (SGI-1776 and ETP-45299) and one new natural product-derived PIM1 inhibitor (tryptanthrin) to induce radiosensitizing activity in NSCLC cells. Lead compounds for developing inhibitors specific for PIM1 may exert therapeutic effects for treating primarily radioresistant tumors.

2. Materials and methods

2.1. Chemicals, antibodies, reagents and siRNA transfections

SGI-1776, ETP-45299 and tryptanthrin were obtained from Selleck Chemicals (Houston, TX, USA), BioFocus (Cambridge, UK) and Wako Chemical (Osaka, Japan), respectively. The following antibodies were used for Western blot analysis or immunoprecipitation: anti-Bad, anti-PIM1, anti-tubulin, anti-Lamin A/C, anti-PRAS40, anti-pPRAS40 (Thr246), anti-Hemagglutinin (HA), anti-pan-14-3-3, anti-FOXO3a, anti-pFOXO3a (Thr32 and Ser253), anti-pAKT (Thr308 and Ser473), anti-AKT, anti-Bim, and anti-FasL antibodies (from Santa Cruz, CA or Cell Signaling Technology, Beverly, MA). Protein-A sepharose was acquired from Calbiochem (San Diego, CA). Cell culture media (RPMI-1640), fetal bovine serum (FBS), glutamine, penicillin, streptomycin and Trizol® were acquired from Gibco (Grand Island, NY). siRNA oligonucleotides targeting PIM1 and AKT (ON-TARGETplus siRNAs) were obtained from Dharmacon (Chicago, IL). Cells were seeded in 6-well dishes and transfected with 100 ng of the siRNA oligonucleotides, using DharmaFECT 1 (Dharmacon) following the manufacturer's instruction.

2.2. Cell lines, cell culture and irradiation

We obtained A549 NSCLC cells, a representative of adenocarcinomas from the American Type Culture Collection (ATCC, Manassas, VA). The cells were grown in RPMI-1640 medium supplemented with 10% FBS, 100 U/ml penicillin, and 100 μg/ml streptomycin at 37 °C in 95% air/5% CO_2. For irradiation, cells were plated in a 75-cm^2 cell culture flask, allowed to grow to ~60–80% confluence, and then irradiated with a single dose of γ-rays under ambient conditions. All irradiation procedures were performed using a Gamma Cell 40 Exactor (Nordion International, Inc., Ottawa, Canada) at a dose rate of 0.81 Gy/min. Flasks containing the control cells were placed in the irradiation chamber but not exposed to radiation.

2.3. Screening of PIM1 inhibitor candidates

In silico studies were performed using the program suite Schrödinger (http://www.schrodinger.com). A number of known PIM1 inhibitors and polyphenol compounds were noted from a published source describing some bioactive compounds and their potential use in the treatment of various diseases. The structures of these compounds were collected from the PubChem database

(http://pubchem.ncbi.nlm.nih.gov) and the geometries were optimized using LigPrep module with OPLS-2005 as force field. The atomic coordinates of PIM1 was downloaded from Protein Data Bank (PDB ID: 1XR1; http://www.pdb.org) and the crystallographic water molecules were excluded prior to the energy minimization. The protein structure was then prepared using protein preparation wizard workflow as follows: adding hydrogen, assigning partial charges using OPLS-2005 force field and incorporating protonation states. The minimized structure was further used for screening and docking studies. The scaling factor of protein van der Waals radii for the receptor grid generation was set as 0.8 Å. Extra Precision (XP) method implemented in glide module was applied for the screening process and the minimized compounds were docked to the grid volume. Based on the glide score, compounds were filtered and three compounds were selected for the *in vitro* analysis. The literature survey also indicated that the compound is very promising for further study.

2.4. Thiazolyl blue tetrazolium bromide assay (cell viability assay)

A549 cells were seeded and cultured in a 24-well plate with or without different concentrations of PIM1 inhibitors for 4 h. Media were removed, a 0.05% thiazolyl blue tetrazolium bromide solution (Sigma, St. Louis, MO) was added, and the cells were incubated at 37 °C for 2 h. Next, the thiazolyl blue tetrazolium bromide solution was replaced with dimethyl sulfoxide (DMSO) and the plates were incubated for 10 min. After incubation, the solution was transferred to a 96-well plate in duplicate and the absorbance was measured.

2.5. Isothermal titration calorimetry (ITC)

His-PIM1 was generated as previously described [31]. Direct interaction between PIM1 and a selected PIM1 inhibitor was measured using a MicroCal VP-ITC instrument (GE Healthcare, Pittsburgh, PA) at 25 °C following standard procedures. Recombinant His-PIM1 was equilibrated with 20 mM Tris buffer (pH 7.5) containing 150 mM NaCl. Protein was added to the calorimetric reaction cell at a concentration of 0.01 mM and titrated with 0.1 mM PIM1 inhibitor in the same buffer. Protein and ligand solutions were degassed prior to use. Each titration experiment was performed with 29 injections of 10 μl at 300-s equilibration intervals. Heat of dilution for an individual ligand was determined by titration of the ligand into the same buffer without protein and used for correction of the protein titration. Data were fitted to a single-site binding model by non-linear least-square regression using the Origin software package. The fit of data yielded the binding affinity (K_d), enthalpy change (ΔH), entropy change (ΔS), and binding stoichiometry for the titration.

2.6. Western blot analysis, immunoprecipitation, and transient transfection

Following the desired treatments, cell (5×10^6 cells) lysates were prepared using RIPA buffer (50 mM Tris, pH 7.4, 150 mM NaCl, 1% Triton X-100, 25 mM NaF, 1 mM DTT, 20 mM EGTA, 1 mM Na_3VO_4, 0.3 mM phenylmethylsulfonyl fluoride (PMSF), and 5 U/ml aprotinin). To prepare the nuclear protein extracts, the cells were harvested and collected by centrifugation. Cells were suspended in buffer A (10 mM HEPES, pH 7.9, 50 mM NaCl, 1 mM DTT, 0.1 mM EDTA, and protease inhibitors) for 20 min on ice. An equal volume of buffer B (250 mM sucrose, 1 mM EDTA, 10 mM Tris–HCl, pH 7.5, protease inhibitor AEBSF, and 0.1% NP-40) was then added and the suspension was allowed to sit for 20 min on ice. Following centrifugation, the supernatant (cytosol fraction) was collected and centrifuged at 5,000 × *g* for 2 min to remove cellular debris. The nuclear pellet was washed two times with buffer A, and resuspended in buffer C (10 mM HEPES, pH 7.9, 400 mM NaCl, 1 mM DTT, 1 mM EDTA, and 1 mM EGTA). Nuclear fractions were cleared of debris by centrifugation at 12,000 × *g* for 15 min at 4 °C. Protein concentration of the lysates was determined using a Bio-Rad protein assay kit (Bio-Rad Laboratories, Hercules, CA). Western blot analysis and immunoprecipitation studies were performed as described previously [7].

For transient transfection, cells were plated at a density of 5×10^5 cells in 6-well dishes and incubated for 4 h for stabilization. Cells were transiently transfected with 2.5 μg of the indicated plasmid using Lipofectin (Gibco), a transfection reagent, according to instructions supplied by the manufacturer.

2.7. Northern blot analysis

Following the desired treatments, total cellular RNA was isolated from cells (3×10^6 cells) using Trizol®. Total cellular RNA was electrophoresed on a 1.2% agarose gel containing formaldehyde and transferred to nylon membranes. Following UV cross-linking, membranes were prehybridized for 30 min in ExpressHyb Hybridization solution and hybridized for 4 h at 65 °C with radiolabeled DNA probes specific for human *Pim1* cDNA (sense: 5'-CAA CGA CCT GCA ACG CCA C-3', antisense: 5'-AGA GAC CCT CTG CCT GAA G-3'). The *Pim1* probes were labeled with [α-^{32}P] CTP using a random priming kit. Following hybridization, membranes were washed twice for 10 min at room temperature, first in 1× SSC and then 0.1% DS solution. The washed membranes were then subjected to autoradiography.

2.8. In vitro and in vivo kinase assay

Kinase assays were carried out as previously described [7]. For the *in vitro* kinase assay, A549 cell lysates were prepared in RIPA buffer. Aliquots of the lysates were immunoprecipitated overnight with the indicated specific antibody and then incubated for 4 h with protein-A sepharose beads (50 μl per sample) (Invitrogen, Carlsbad, CA). The beads were washed with RIPA buffer three times, and then incubated with His-tagged target proteins (Bad or PRAS40) in the presence of [γ-^{32}P] ATP (10 μCi) (PerkinElmer Life Sciences, Boston, MA) and 30 μl of kinase buffer (20 mM Tris, pH 7.5, and 10 mM $MgCl_2$) for 30 min. The reaction was stopped by addition of 4× SDS sample buffer and boiling for 5 min. Samples were subjected to SDS-PAGE and analyzed by autoradiography to monitor phosphorylation of the target proteins by PIM1. For the *in vivo* kinase assay, A549 cells were transfected with HA-PRAS40 for 24 h and then irradiated. Aliquots of the lysates were immunoprecipitated overnight with anti-HA antibody. Western blot analysis was performed using phospho-specific antibody.

2.9. Luciferase reporter gene assay

Following overnight transfection, the medium was changed and treated with irradiation. After 1 h, the cells were washed twice with cold PBS and lysed in reporter lysis buffer (Promega, Madison, WI). After vortexing the lysates and centrifugation at 12,000 × *g* for 1 min at 4 °C, 20 μl of the cell extract and 100 μl of luciferase assay reagent were mixed at room temperature, and placed in a luminometer (AutoLumat LB 953, EG & G Berthold, Bad Widbad, Germany) to measure luciferase activity in the solution.

2.10. Chromatin immunoprecipitation (ChIP)

Following overnight transfection with specific PIM1 inhibitors and irradiation as indicated, 5×10^8 cells expressing FLAG-FOXO3a were cross-linked in 1% formaldehyde, quenched in 125 mM glycine and washed twice in chilled PBS. Cells were then lysed in a solution containing 1% SDS, 10 mM EDTA, 50 mM Tris, pH 8.1, and

protease inhibitors, and sonicated in 30-s pulses with 30-s intervals of rest. The sonicated lysates were centrifuged for 10 min at maximum speed and diluted 5-fold in dilution buffer (0.01% SDS, 1.1% Triton X-100, 1 mM EDTA, 20 mM Tris–HCl, pH 8.1, and 200 mM NaCl). To reduce unspecific binding during immunoprecipitation, the diluted lysates were precleared using protein-A/G Plus agarose and calf thymus DNA at 4 °C for 1 h. Immunoprecipitation was performed with anti-FLAG or anti-IgG antibody. Immune-complexes were collected and washed in chilled low salt buffer (0.1% SDS, 1% Triton X-100, 2 mM EDTA, 20 mM Tris–HCl, pH 8.1, and 150 mM NaCl), high salt buffer (low salt buffer containing 500 mM NaCl), and LiCl wash buffer (0.25 M LiCl, 1% Nonidet P-40 1% deoxycholate, 1 mM EDTA, and 10 mM Tris–HCl, pH 8.1), and then washed twice in 10 mM Tris/5 mM EDTA. DNA was extracted twice from the beads using 100 μl of elution buffer (1% SDS and 0.1 M NaHCO) and supplemented with 0.25 M NaCl. Following an overnight incubation at 65 °C to reverse cross-linking, the samples were incubated for an additional hour at 65 °C with 10 μM EDTA, 40 μM Tris, pH 6.8, and 2 μg of proteinase K. DNA was purified using a QIAquick PCR purification kit (Quiagen, Hilden, Germany) for PCR. PCR was performed with primers that encompassed regions containing the *Bim* and *FasL* gene promoters. The following primers were used: *Bim*, 5'-GGG CGG GTA CAT TCT GAG T-3', 5'-CAG GCT GCG ACA GGT AGT G-3'; *FasL*, 5'-GGT ATC CAG CGC TGA TTT GCT-3', 5'-ACC TCT CTC CAG TTC TCT TCT-3'.

2.11. Apoptosis assay

Apoptosis induction was assessed by analyzing cytoplasmic histone-associated DNA fragmentation. In brief, cells were plated at a density of 4×10^5 cells in 96-well plates and allowed to attach overnight. Cells were then exposed to desired treatment (IR and/or PIM1 inhibitors). Cytoplasmic histone-associated DNA fragmentation was monitored using a cell death detection kit (Roche Applied Science, Mannheim, Germany) according to the manufacturer's instructions [32].

2.12. Tumor xenografts in nude mice

Six-week-old male BALB/c athymic nude mice (Central Lab Animals Inc., Seoul, South Korea) were used for the *in vivo* experiments. The protocols used were approved by the Institutional Animal Care and Use Committee of Pusan National University, and performed in accordance with the provisions of the NIH Guide for the Care and Use of Laboratory Animals. The animals were fed water and a standard mouse chow diet *ad libitum*. Animals were injected with 2×10^6 A549 cells into the flank and tumors were allowed to develop. Upon identification of a palpable tumor (minimal volume of 200 mm^3), DMSO or PIM1 inhibitor (200 μg/kg body weight) was administered intraperitoneally every day for 25 d. The animals were also irradiated with 10 Gy once a week for 3 weeks. Tumor length (L) and width (l) were measured with a caliper and tumor volumes were calculated with the formula $(L \times l^2)/2$. At the end of the treatment period, the animals were euthanized and the tumors were used for biochemical studies

2.13. Statistical analysis

All numeric data are presented as the mean ± standard deviation (SD) from at least three independent experiments, and were analyzed using the one-way ANOVA on ranked data followed by a Tukey's honestly significant difference test, and the two-way ANOVA on ranked data followed by a Bonferroni post test. Prism 4 software (GraphPad Software, San Diego, CA) was used to conduct all statistical analyses. A p-value < 0.05 was considered statistically significant.

Table 1
PIM1 binding parameters determined by isothermal titration calorimetry (ITC).

Compounds	K_d/μM	ΔH/kcal mol^{-1}	ΔS/cal mol^{-1} $degree^{-1}$
SGI-1776	18 ± 1.2	−18.9 ± 1.1	−51.3
ETP-45299	14 ± 0.8	−21.1 ± 0.9	−24.5
Tryptanthrin	25 ± 1.1	−22.3 ± 0.8	−61.3

3. Results

3.1. Identification of PIM1 inhibitors as candidates of radiosensitizers

Based on the function of PIM1 in radioresistance from our previous work, we hypothesized that PIM1-specific inhibitors could induce radiosensitization in NSCLC cells [7]. The X-ray crystal structure of PIM1 kinase in complex with AMP-PNP (PDB ID: 1XR1) was used for reference coordinates in the creation of a model for virtual screening [22]. A large number of known PIM1 inhibitors and polyphenol compounds were then prepared for screening. Predictive calculations of pharmaceutical properties were used to select compounds. Virtual hits from this screen were evaluated and refined so that approximately 20 structures were selected. These were further evaluated and analyzed according to criteria for solubility and molecular weight along with Lipinski-like criteria that narrowed the hits to three compounds as candidates for further development: SGI-1776 and ETP-45299 (among known PIM1 inhibitors) and tryptanthrin (among polyphenol compounds) (Fig. 1A).

An ITC experiment was next performed to compare the binding parameters between purified PIM1 and selected inhibitors. Measurement of the heat that is generated or absorbed upon ligand-binding by ITC allows accurate determination of the binding constant (K_a) as well as enthalpy and entropy changes, thereby providing a complete thermodynamic profile of the molecular interaction. In every case, calorimetric data revealed that heat was released when pure inhibitors were individually associated with PIM1, indicating that these interactions made significant enthalpic contributions to binding (Table 1). ITC findings also revealed slightly unfavorable entropic contributions for each, possibly indicating that PIM1 was slightly stabilized upon binding. This effect was especially noticeable for the inhibitors, possibly promoted by the significant reduction of B-values of the binding pocket upon formation of a binary complex. ITC showed that PIM1 binds substrates with a stoichiometry of 1:1, indicating that the protein concentration could be determined with reasonable accuracy and that the protein was properly folded. As shown in Table 1, SGI-1776, ETP-45299 and tryptanthrin had dissociation constants of 18 ± 1.2, 14 ± 0.8 and 25 ± 1.1 μM, respectively. On the other hand, other compounds that have similar flat, multiring structures and molecular masses, such as $NADP^+$, ATP, and tryptophan, failed to show any significant binding to PIM1, judging from the ITC signals.

To determine the concentration of PIM1 inhibitors that can be used without affecting cell viability, A549 cells (a representative radioresistant lung adenocarcinoma cell line) were treated with PIM1 inhibitor at different concentrations or DMSO as a vehicle control for 4 h (Fig. 1B). SGI-1776, ETP-45299, or tryptanthrin did not affect cell viability up to concentrations of 15 μM, 15 μM, or 20 μM, respectively, and noncytotoxic concentration of these inhibitors used in this study was determined.

To confirm whether selected three PIM1 inhibitors can reduce PIM1 kinase activity, we performed an *in vitro* kinase assay with purified recombinant His-tagged PIM1 protein and HA-tagged

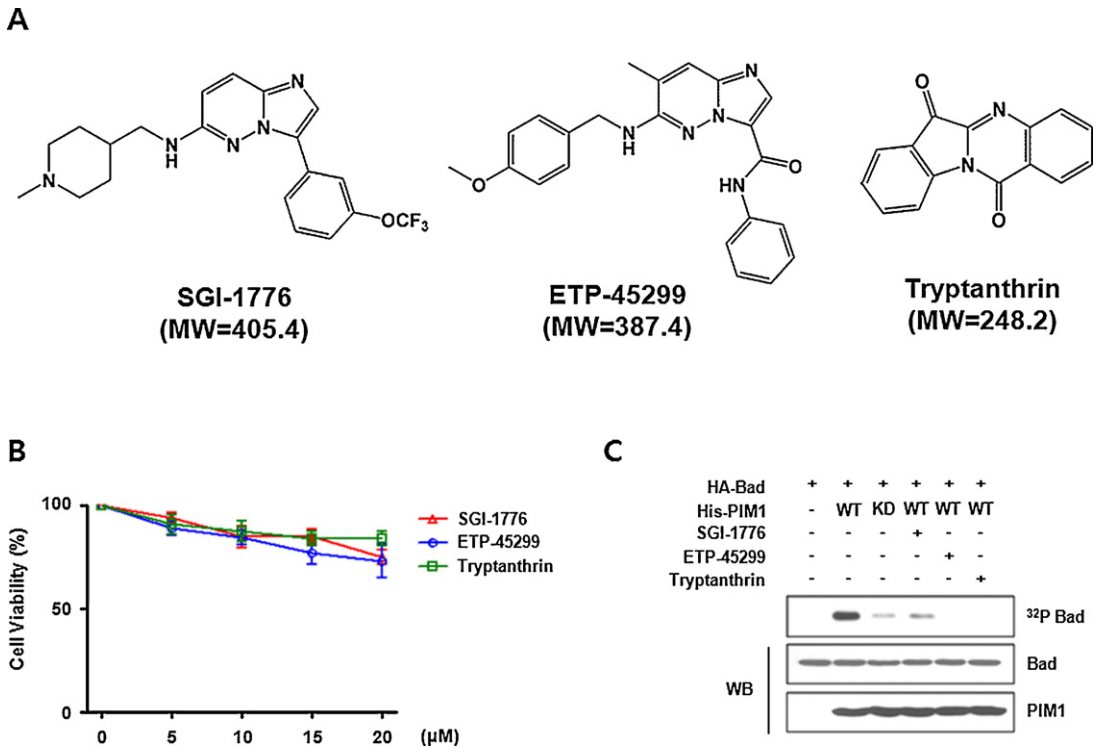

Fig. 1. Identification of PIM1 inhibitors as candidates of radiosensitizer. (A) Chemical structures of the selected PIM1 inhibitors. (B) Effects of the PIM1 inhibitors on the viability of A549 cells were measured by triazolyl blue tetrazolium bromide assay. Cells were treated with the indicated inhibitors at concentrations up to 20 μM for 4 h. Absorbance was measured at 570 nm. All experiments were done in triplicate and the data are presented as the mean ± SD. (C) The effect of PIM1 inhibitors on PIM1 kinase activity was measured by *in vitro* kinase assay. HA-tagged Bad was immunoprecipitated from the lysates of A549 cells treated with or without PIM1 inhibitors, and used as substrate for the PIM1 kinase assay that measures [γ-^{32}P] ATP incorporation. His-tagged PIM1 was expressed in *Escherichia coli* and affinity purified before use in the kinase assay. Phosphorylated proteins were separated by SDS–PAGE and visualized by autoradiography. Upper panel shows Bad phosphorylation, whereas the middle and lower panels of the Western blot analysis show the amount of HA-tagged Bad and PIM1 loaded onto the gel, respectively.

Bad, a well-known target of PIM1, immunoprecipitated with anti-HA antibody from lysates of transfected A549 cells (Fig. 1C). Results of the assay demonstrated that all selected PIM1 inhibitors significantly suppressed PIM1 kinase activity *in vitro*. Taken together, these findings indicate that the selected compounds significantly inhibited PIM1 activity and may possibly serve as lead compounds for drug development in PIM1 mediated pharmacology.

3.2. PIM1 inhibitors block PIM1-mediated phosphorylation of PRAS40 in radioresistant NSCLC cells

Our previous study has suggested that IR increases the expression of PIM1 at both the mRNA and protein levels, and also nuclear localization of PIM1 in radioresistant A549 cells [7]. To determine whether IR-induced PIM1 expression and nuclear localization could be regulated by the selected PIM1 inhibitors, A549 cells were treated with PIM1 inhibitors and 2 Gy (the dose commonly used in radiation biology experiments) of IR for 1 h.

Exposure to IR dramatically induced *Pim1* mRNA and PIM1 expression in the cells, and no marked decrease in *Pim1* mRNA or PIM1 expression was noted after treatment with inhibitors (Fig. 2A and B). In addition, IR caused a marked increase of PIM1 nuclear localization in the A549 cells and this was not noticeably reduced by pre-incubation with PIM1 inhibitors (Fig. 2C). Taken together, these data suggest that the selected PIM1 inhibitors did not block not only PIM1 expression but also nuclear localization of PIM1 in IR-treated A549 cells.

Since we found that neither PIM1 expression nor localization was altered by the selected inhibitors, we further examined the effect of the inhibitors on kinase activity of PIM1 in IR-induced radioresistant NSCLC cells. PIM1 has been shown to directly phosphorylate PRAS40 on Thr246 both *in vitro* and *in vivo* [7,33,34]. To determine whether the phosphorylation of PRAS40 (especially on Thr246) by PIM1 is blocked by the inhibitors, we performed an *in vitro* kinase assay with purified recombinant His-tagged PIM1 protein (WT or KD) and HA-tagged PRAS40 immunoprecipitated with anti-HA antibody from transfected A549 cells treated with or without the inhibitors (Fig. 2D). For the *in vivo* kinase assay, A549 cells were transfected with a vector expressing FLAG-tagged PIM1 for 24 h. The cells were harvested and fractionated 4 h after treatment with the inhibitors and 1 hr after irradiation. The phosphorylation status of PRAS40 on Thr246 in the nucleus was determined with a phospho-specific antibody (Fig. 2E). While a high level of PRAS40 Thr246 phosphorylation was observed in cells transfected with PIM1 and WT PRAS40, a significantly lower level of phosphorylation was detected following treatment with the inhibitors. These results demonstrate that the selected PIM1 inhibitors directly blocked the phosphorylation of PRAS40 Thr246 induced by IR-activated, nuclear localized PIM1.

3.3. PIM1 inhibitors block complex formation of pPRAS40, pFOXO3a, and 14-3-3, and reduce cytoplasmic retention of FOXO3a in radioresistant NSCLC cells

Since we found that phosphorylation of PRAS40 by IR-activated PIM1 in the nucleus of radioresistant NSCLC cells was blocked by PIM1 inhibitors, we further examined the effects of these inhibitors on PRAS40-mediated nucleus events. Data from a previous study demonstrated that PIM1-mediated pPRAS40, 14-3-3, and AKT-mediated pFOXO3a form a trimeric complex in radioresistant NSCLC cells [7,35]. The best described mechanism responsible

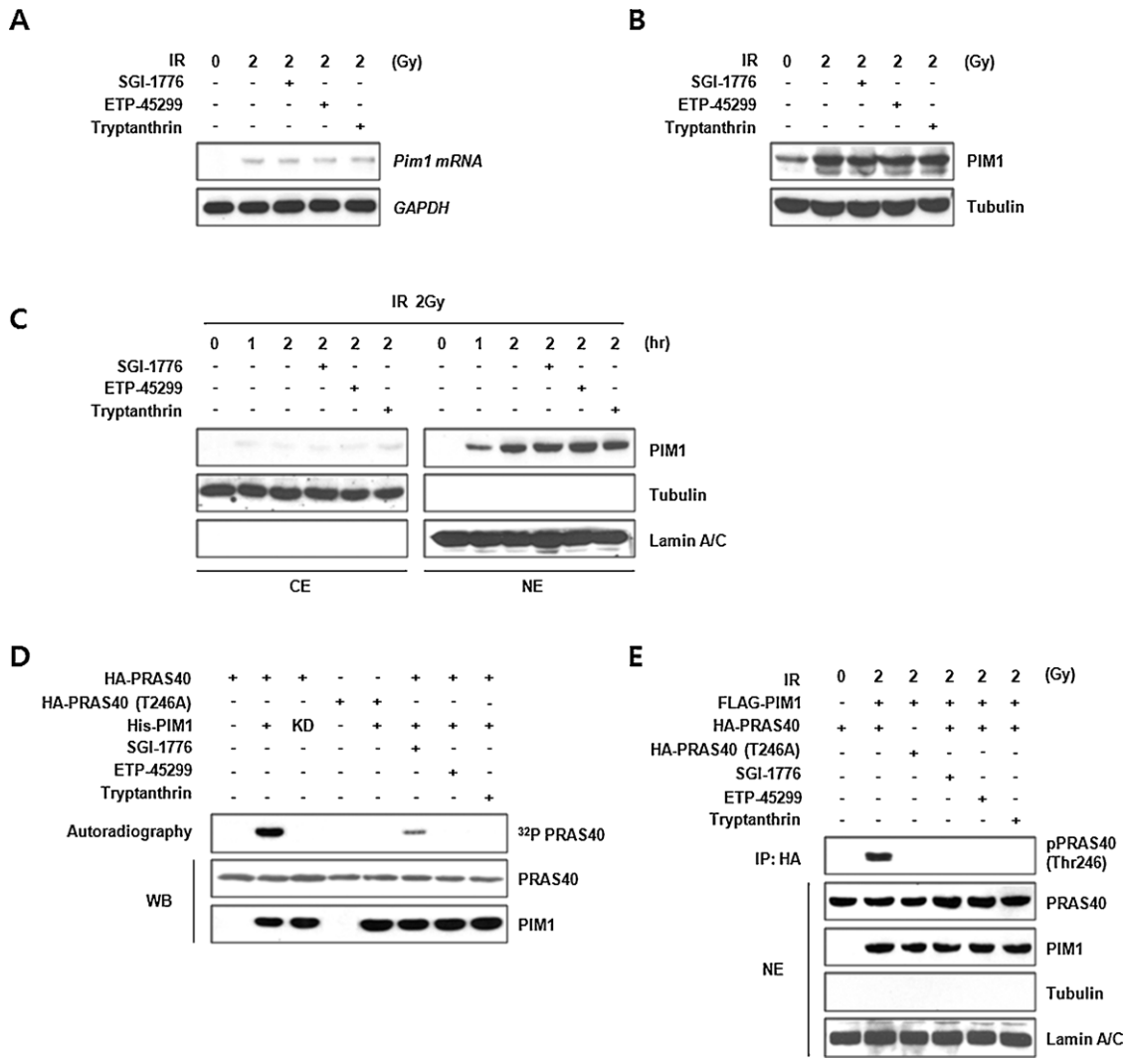

Fig. 2. PIM1 inhibitors block PIM1-mediated phosphorylation of PRAS40 in radioresistant NSCLC cells. (A) The effect of PIM1 inhibitors on IR-induced *Pim1* mRNA expression in A549 cells was assessed by Northern blot analysis. Total RNA (15 μg) was analyzed using an [α-^{32}P]-labeled *Pim1* cDNA probe. GAPDH was used for normalization. (B) The effect of PIM1 inhibitors on IR-induced PIM1 expression was detected by Western blot analysis. After treatment with PIM1 inhibitors and irradiation, A549 cells were harvested and the cell lysates were subjected to analysis with antibody against PIM1. (C) The effect of PIM1 inhibitors on IR-induced PIM1 translocation into the nucleus was assayed by Western blot analysis. CE: cytoplasmic extract; NE: nuclear extract. (D) The effect of PIM1 inhibitors on PRAS40 phosphorylation by PIM1 was measured by *in vitro* kinase assay as described in the legend for Fig. 1C. Either HA-tagged PRAS40 or PRAS40-T246A mutant protein immunoprecipitated from the cell lysates was used as substrate for His-tagged PIM1. (E) The effect of PIM1 inhibitors on the phosphorylation of PRAS40 at Thr246 by PIM1 *in vivo* was measured by *in vivo* kinase analysis. To induce overexpression of PIM1, A549 cells were transfected with FLAG-tagged PIM1 for 24 h. After treatment with PIM1 inhibitors and irradiation, HA-tagged PRAS40 WT or T246 mutants was immunoprecipitated from the lysates using an anti-HA antibody, and then Western blot analysis was performed. Phosphorylation of PRAS40 was detected by a phospho-specific antibody.

for the functional activity of FOXO3a is phosphorylation followed by translocation into the cytoplasm. Phosphorylation of nuclear FOXO3a on three evolutionarily conserved residues (Thr32, Ser253, and Ser315) by AKT promotes FOXO3a sequestration in a cytoplasmic compartment [36]. In addition, the binding of 14-3-3 to pThr32 and pSer253 likely contributes to cytoplasmic sequestration of FOXO3a by masking the nuclear localization signal (NLS) from the nuclear import machinery [37]. Therefore, we evaluated the effect of PIM1 inhibitors on the complex formation of pPRAS40, 14-3-3, and pFOXO3a in radioresistant NSCLC cells. As shown in Fig. 3A, complex formation of pPRAS40 with endogenous 14-3-3 and FOXO3a was detected. However, the trimeric complex was not detected in PIM1 inhibitor-treated cells, thus suggesting the involvement of PIM1 kinase activity in formation of the trimeric complex (Fig. 3A).

Next, we examined the effect of the PIM1 inhibitors on the kinetics of PRAS40/14-3-3/FOXO3a translocation in radioresistant NSCLC cells. As shown in Fig. 3B, stimulation of A549 cells with 2 Gy of IR led to rapid phosphorylation of endogenous PRAS40 and FOXO3a as well as translocation of these proteins with 14-3-3 from the nucleus to the cytoplasm. In contrast, the translocation and cytoplasmic retention of FOXO3a was not detected in PIM1 inhibitor-treated radioresistant cells. These results demonstrate that the selected PIM1 inhibitors directly blocked the formation of pPRAS40, 14-3-3 and pFOXO3a complexes along with concomitant cytoplasmic retention of FOXO3a in radioresistant cells.

3.4. PIM1 inhibitors increase apoptosis and radiosensitivity of radioresistant NSCLC cells

Several studies have revealed that radiation-induced apoptosis promoted by the expression of pro-apoptotic genes regulates radiosensitivity in several types of cancer cells [7,38,39]. In an attempt to compare the transcriptional activity of FOXO3a on

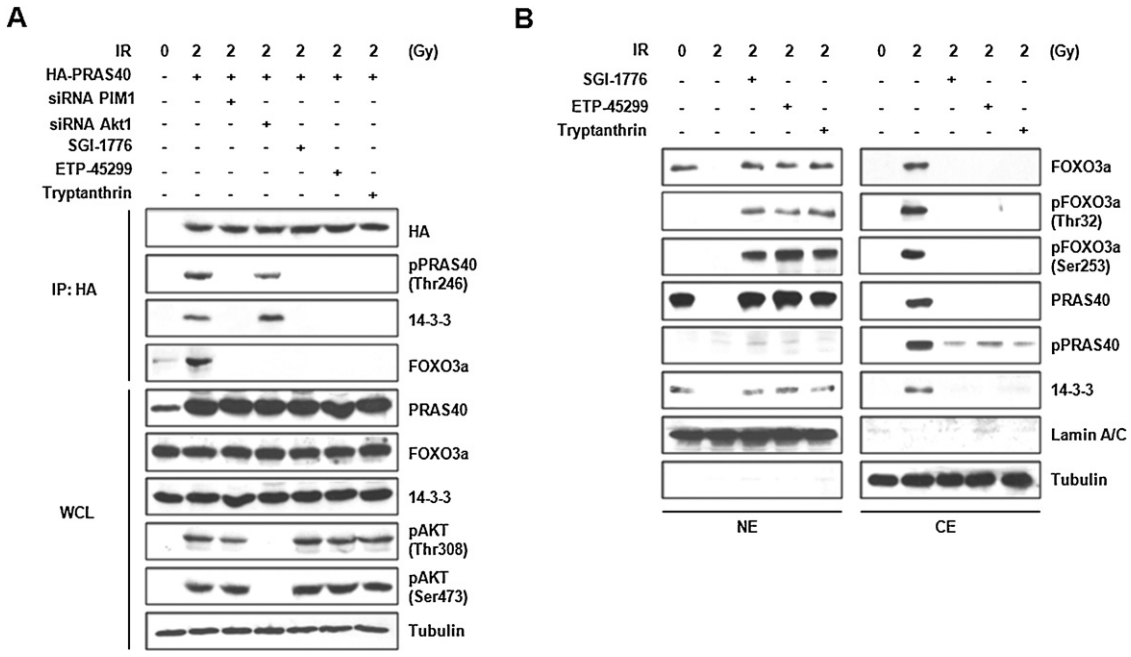

Fig. 3. PIM1 inhibitors block complex formation of phospho-PRAS40, phospho-FOXO3a and 14-3-3 and reduce cytoplasmic retention of FOXO3a in radioresistant NSCLC cells. (A) The effect of PIM1 inhibitors on trimeric complex formation of pPRAS40, pFOXO3a, and 14-3-3 *in vivo* was measured by immunoprecipitation and Western blot analysis. For overexpression of PRAS40, A549 cells were transfected with HA-tagged PRAS40 for 24 h. Cells were pretreated with PIM1 inhibitors and then exposed to 2 Gy of IR. After another hour, HA-tagged PRAS40 was immunoprecipitated from cell lysates using an anti-HA antibody and analyzed by Western blotting with anti-HA, anti-pPRAS40 (Thr246), anti-pan-14-3-3, and anti-FOXO3a antibodies. Total levels of PRAS40, FOXO3a, 14-3-3, pAKT (Thr308/Ser473), and tubulin were measured by Western blot analysis with specific antibodies. (B) The effect of PIM1 inhibitors on the kinetics of PRAS40/14-3-3/FOXO3a subcellular translocation was measured by Western blot analysis. Following treatment with the PIM1 inhibitors and exposure to 2 Gy of IR, cell lysates were collected, fractionated and then subjected to Western blot analysis with the indicated antibodies.

pro-apoptotic genes between PIM1 kinase-treated and untreated radioresistant cells, A549 cells were transfected with a luciferase reporter plasmid containing the FOXO response element of the TNF-related apoptosis-inducing ligand promoter region, FLAG-tagged FOXO3a or FLAG-tagged FOXO3a-3mut that is impervious to AKT-mediated phosphorylation. Treatment with PIM1 inhibitors and IR (2 Gy) increased FOXO-luciferase activity approximately by 3.0-fold in the A549 cells compared to the untreated control, suggesting that cellular localization-dependent transcriptional activity of FOXO3a induced by PIM1-mediated phosphorylation of PRAS40 and formation of the trimeric complex affects NSCLC cell radiosensitivity (Fig. 4A).

To investigate the correlation between the effect of PIM1 inhibitors and radioresistance in A549 cells, we next determined whether FOXO3a may bind to FOXO-response element (FRE) sequences in *Bim* and *FasL*, two FOXO3a-regulated pro-apoptotic genes, after treatment with the PIM1 inhibitors [40]. For this, we performed a ChIP analysis to measure the binding of FLAG-tagged FOXO3a at the *Bim* and *FasL* loci. As shown in Fig. 4B, an increased association between FOXO3a and each FRE locus was detected following treatment with the PIM1 inhibitors. Concomitantly, the expression levels of Bim and FasL were also increased by blocking PIM1 activity (Fig. 4C).

To further confirm whether PIM1 inhibition functionally influence radioresistance in NSCLC cells, an apoptosis assay was performed. Compared to untreated A549 cells, PIM1 inhibitor-treated cells were more sensitive to IR-mediated cytoplasmic histone-associated DNA fragmentation, a measure of apoptotic cell death (Fig. 4D). Moreover, silencing PIM1 and AKT expression with siRNA significantly increased apoptosis in IR-irradiated A549 cells. These results suggested that inhibition of PIM1 kinase activity by the PIM1 inhibitors as well as expression of downstream signaling molecules were functional regulatory point of cell death and radioresistance in NSCLC cells.

3.5. PIM1 inhibitors increase in vivo sensitization to radiation in a xenograft mouse model

To evaluate the combined effects of the PIM1 inhibitors and IR on tumor growth *in vivo*, a xenograft mouse model was designed (Fig. 5A). *In vivo* data from nude mice bearing tumors formed by A549 radioresistant cells indicated that PIM1 inhibitors had an *in vivo* radiosensitization effect (Fig. 5B). Tumor volume of mice treated with IR and PIM1 inhibitors on day 25 was significantly reduced by approximately 46, 61, and 42% in animals treated with SGI-1776, ETP-45299 and tryptanthrin, respectively, compared to mice receiving IR alone. In addition, when PIM1 inhibitors were directly administered at the tumor site in the mice, IR-induced phosphorylation of PRAS40 was not detected in the extracted tumor tissue lysates (Fig. 5C). Moreover, the amount of cytoplasmic retention of FOXO3a in the tumor tissue lysates was dramatically reduced by treatment with the PIM1 inhibitors (Fig. 5D). Thus, we suggest that the three PIM1 inhibitors we evaluated have a potent radiosensitization effect *in vivo*.

4. Discussion

In this study, we determined the radiosensitizing activity of SGI-1776, ETP-45299, and tryptanthrin targeting PIM1 activity. These potential radiosensitizers disrupt formation of a trimeric complex between PRAS40, 14-3-3, and FOXO3a through inhibition of PRAS40 phosphorylation and consequently promote FOXO3a transcriptional activity for the expression of proapoptotic protein in radioresistant A549 cells. We found that these three compounds,

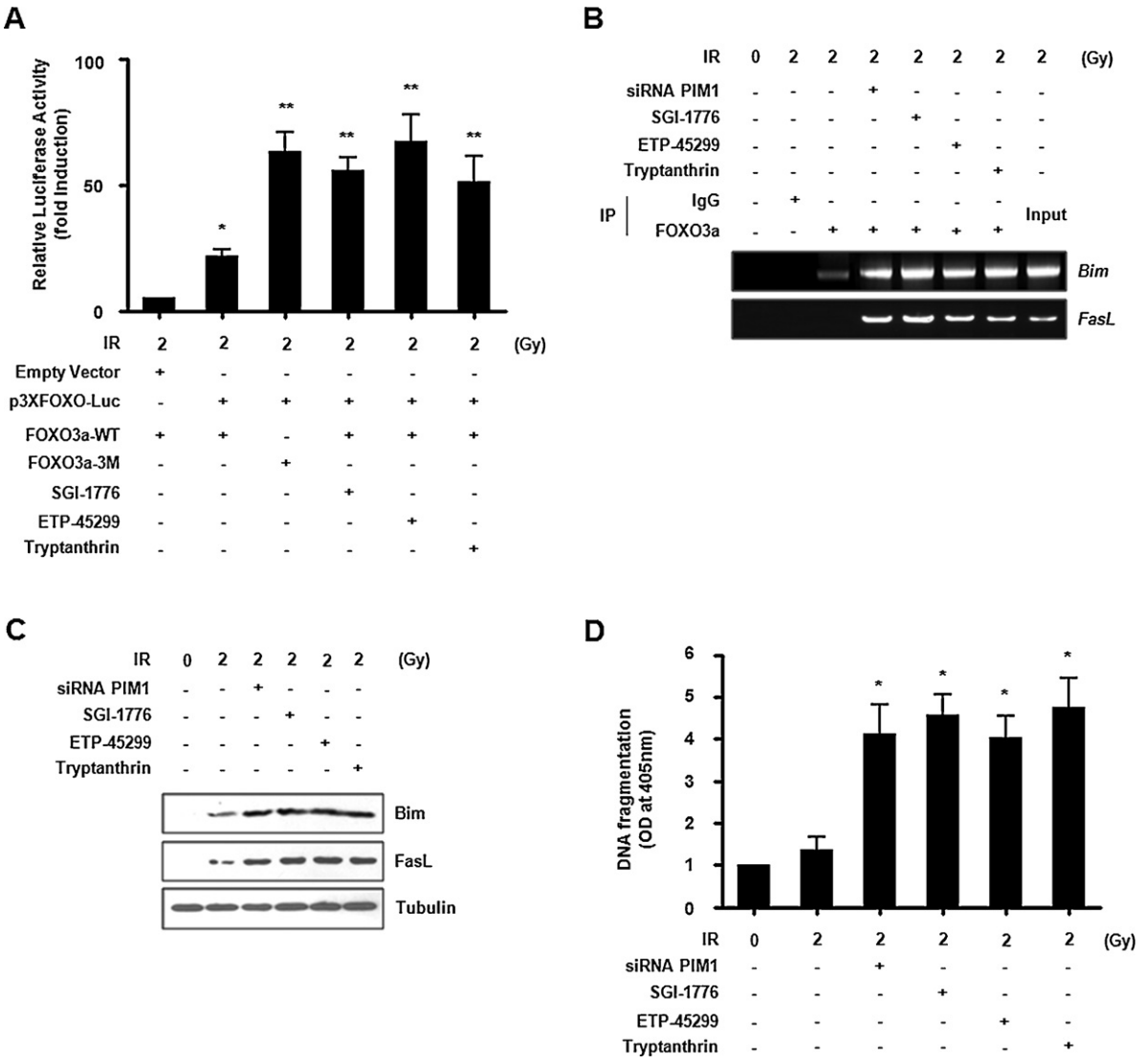

Fig. 4. PIM1 inhibitors increase apoptosis and radiosensitivity of radioresistant NSCLC cells. (A) The effect of PIM1 inhibitors on the transcriptional activity of FOXO3a in NSCLC cells was measured by a reporter gene assay. Cells were co-transfected with 2.5 μg of 3× FOXO luciferase reporter gene plasmid and wild type FLAG-tagged FOXO3a or FLAG-tagged FOXO3a-3 M mutant, allowed to recover for 24 h, and then treated with PIM1 inhibitor and irradiation, as indicated. Cells were harvested at 1 h after treatment, and luciferase activities were measured. The indicated luciferase activities are relative to the β-galactosidase activity of each protein extract. Cells transfected with an empty vector (EV and pGL-3) was used as a control. Data represent the mean ± SD. $^{*}p < 0.05$; EV-transfected cells *versus* 3× FOXO Luciferase reporter gene plasmid-transfected cells, $^{**}p < 0.05$; FLAG-tagged FOXO3a-transfected cells *versus* FLAG-tagged FOXO3a-3 M mutant-transfected cells or each inhibitor-treated cells. (B) The effect of PIM1 inhibitors on the binding of FOXO3a to FRE of *Bim* and *FasL* promoters was measured by ChIP analysis. A549 cells were transfected with specific PIM1 inhibitors, allowed to recover for 24 h, then treated with IR, as indicated, and harvested for ChIP analysis. Chromatin-bound DNA was immunoprecipitated with an anti-FOXO3a antibody. 10% of the chromatin samples were used as a positive control (Input). (C) The effect of PIM1 inhibitors on the expression of Bim and FasL in A549 cells was measured by Western blot analysis. A549 cells treated with IR and/or PIM1 inhibitors were harvested, and the cell lysates were subjected to analysis with antibodies specific for Bim and FasL. (D) The effect of PIM1 inhibitors on PIM1-mediated cell death in NSCLC cells was measured by an apoptosis assay. Analysis of cytoplasmic histone-associated DNA fragmentation in NSCLC cells treated with PIM1 inhibitor and/or IR was performed as indicated. Data represent the mean ± SD. $^{*}p < 0.05$; IR-irradiated A549 cells *versus* IR-irradiated A549 cells treated with siRNA or each inhibitor.

at nontoxic concentrations, significantly sensitized NSCLC cells to radiation both *in vitro* cell culture system and *in vivo* xenograft tumor mice models. It is very likely that our selected PIM1 inhibitors block the kinase activity of PIM1 and then eventually confer transcriptional activation of FOXO3a to express proapoptitc proteins, leading to enhanced cell death and increased sensitivity to radiation.

SGI-1776 and ETP-45299 are imidazopyridazine derivatives inhibitors targeting PIM1 kinase. In previous studies, imidazo[1,2-*b*]pyridazine was identified as a promising lead scaffold, which was then optimized to improve the potency and selectivity of compounds against the PIM1 target *via* specific modifications based on structure–activity relationship (SAR) studies [29,41–44]. SGI-1776 and ETP-45299 were found to be a potent inhibitor of PIM1 with an IC_{50} of 7 ± 1.9 nM and a K_i^{app} of 30 ± 3 nM, respectively [41,44]. Both have been reported to be associated with potent inhibition of cell signaling pathway and tumorigenesis in several models. These inhibitors exhibited anti-proliferative and pro-apoptotic activities in various human cancer cell lines [41,42,44]. SGI-1776 had been progressed in phase I clinical trials, although it was terminated owing to cardiac toxicity [42,45]. ETP-45299 was specifically developed for high selectivity of PIM1 to significantly reduce cross reactivity with other kinases, including FLT-3, PDGFR1 and KIT, while other imidazopyridazine derivatives showed high reactivity toward such kinases. However, ETP-45299 needs to be modified before being developed as a therapeutic agent owing to its stability

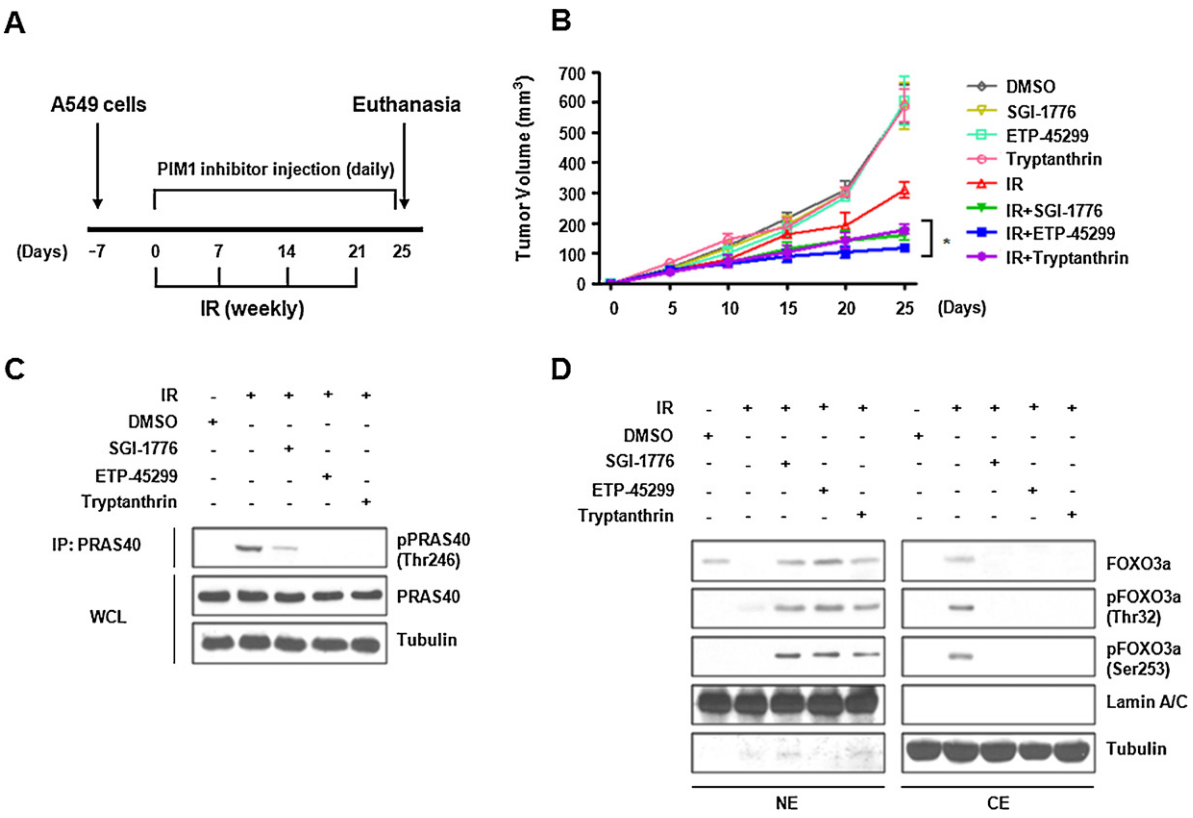

Fig. 5. PIM1 inhibitors exhibit sensitization to the radiation *in vivo* xenografted models. (A) Experimental plan. (B) The *in vivo* effect of PIM1 inhibitors on radiosensitization was measured in mouse *model*. A549 cells were injected in to the flanks of nude mice ($n = 3$ per group) and palpable tumors were allowed to develop for 7 days. Subsequently, PIM1 inhibitor (200 μg/kg body weight) was injected intraperitoneally every day for 25 days. The mice were irradiated (10 Gy) once weekly for 3 weeks. On day 25, tumors were excised and subject to further analyses. Results are expressed as the mean ± SD. $^*p < 0.05$; tumor volume with IR-exposure *versus* tumor volume with IR-exposure and treatment with each inhibitor on day 25. (C) The effect of PIM1 inhibitors on PRAS40 phosphorylation by PIM1 *in vivo* was measured by immunoprecipitation and Western blot analysis. 3 h after the last treatment, tumor tissue samples were obtained. PRAS40 was immunoprecipitated from lysates using an anti-PRAS40 antibody and analyzed by Western blot analysis with an anti-pPRAS40 (Thr246) antibody. Total levels of PRAS40 and tubulin were also measured by Western blot analysis with specific antibodies. (D) The effect of PIM1 inhibitors on the cytoplasmic retention of FOXO3a *in vivo* was measured by Western blot analysis from fractionated tumor tissue samples using the indicated antibodies.

problem [44]. Unlike SGI-1776 and ETP-45299, tryptanthrin is newly identified as a potent PIM1 inhibitor in our investigation. This compound is a naturally occurring phytochemical, and has been reported to have a wide range of biological functions, such as anti-inflammatory, anti-fungal, and anti-bacterial activities [46,47]. Several investigations have determined that tryptanthrin exerts anti-tumor effects on various tumors and shows inhibitory activity toward multiple drug resistance during cancer treatment [47,48]. Although it is very likely that tryptanthrin offers lots of clinically beneficial effects for cancer treatment, its therapeutic efficacy on lung cancer is not fully understood and its correlation with PIM1 and radiosensitizing activity has not been reported. All the small-molecule PIM1 inhibitors that have been reported, including SGI-1776 and ETP-45299, are ATP-binding competitors. These inhibitors can inhibit PIM1 by two distinct binding modes which are ATP mimic binders and non-hinge binders [49]. PIM1 shows unusual conformation of its hinge region that contains a proline residue at position 123 [22]. Due to this proline residue, PIM1 can form only one hydrogen bond in contrast to almost all other protein kinases that generally form two canonical hydrogen bonds with ATP or ATP-mimetic inhibitors. Additionally, PIM1 has extra amino acid residues following proline 123, which create a unique ATP-binding pocket and provide a specific target for drug design [22]. Previous studies have reported that imidazopyridazine derivatives (K00135 and SGI-1776) represented non-hinge binders distinguished by an absence of canonical hydrogen bond formed with the hinge region [29,43,49]. According to the studies, the imidazo[1,2-*b*]pyridazine ring (especially, N5 at the ring) in SGI-1776 form a hydrogen bond with a lysine 67 residue and several hydrophilic functional groups were incorporated into the molecule to enhance the hydrophobic interactions at Leu44, Phe49, Leu120 and other residues [29,43]. This would also provide the information for binding mode of ETP-45299, since these two compounds, as imidazopyridazine derivatives, shared major functional groups, which are responsible for formation of a hydrogen bond and hydrophobic contacts with binding pocket of PIM1. In a similar manner to SGI-1776, ETP-45299 is expected to bind to the opposite side of the hinge region and the nitrogen of the indole ring in ETP-45299 might form a hydrogen bond with the lysine 67 residue in the conserved catalytic site. This interaction would be stabilized by a number of hydrophobic interactions, leading to inhibition of kinase activity. Complex structural analysis of tryptanthrin with any other proteins has not been reported yet, although there are several reports about pharmacological and biological effects of tryptanthrin. Based on complex structural studies about PIM1 and its inhibitors consisting of simple flat ring structures, we have assumed that tryptanthrin might also interact with the ATP-binding pocket of PIM1 [20,50]. The carbonyl oxygen of the indole moiety in tryptanthrin might form a hydrogen bond network with the several residues including Lys67, Glu89, and Asp186 in catalytic sites of PIM1 and a water molecule, like non-hinge binders, because the distance between hinge region and the nitrogen or

carbonyl oxygen of the functional groups in tryptanthrin might not be sufficiently close to form the hydrogen bond. To better understand the precise binding mode, further investigations such as a complex structural analysis between PIM1 and tryptanthrin should be performed. In addition, we monitored in the ITC experiments that tryptanthrin had relatively lower affinity to PIM1 than SGI-1776 and ETP-45299 (Table 1). To improve the potency against targets, a large number of inhibitors have been modified in their specific functional groups based on SAR studies [30,51,52]. Various substituents, including alkyl, O, S, N or cyclic moiety, would be applicable for better inhibitory efficacy of tryptanthrin against PIM1. Considering possibility of further modification based on SAR study, tryptanthrin would be used as a novel lead scaffold to be optimized for much enhanced potency and selectivity against PIM1, even though tryptanthrin itself could sufficiently inhibit PIM1 activity.

Several inhibitors for PIM kinases have been investigated for effects of casein kinase 2 (CK2) inhibition as dual inhibitors because of relatively similar ATP binding site of both kinases [22,53,54]. In addition, similar to PIM1, CK2 is constitutively active, and is highly associated with tumorigenesis and radioresistance [55,56]. According to structural analysis of dual inhibitors for PIM1 and CK2, dual inhibitors tend to be usually flat-form structures and could be occupied in the ATP-binding site by lots of hydrophobic interactions between the aromatic rings of the inhibitors and the several hydrophobic residues near the binding pocket in active site [53,57–59]. These dual inhibitors could also directly interact with Lys67 of PIM1 and Lys68 of CK2, respectively, at the conserved catalytic site leaving the hinge unbound [53]. The described binding mode is similar to characteristic of non-hinge binders of PIM1 inhibition, such as SGI-1776, ETP-45299 and, possibly, tryptanthrin [49]. However, SGI-1776 and ETP-45299 could not be accessible in ATP-binding site of CK2 due to their size and non-flat structures. In the same context, there have been no reported evidence reported about the inhibitory activity of SGI-1776 on CK2 so far, and ETP-45299 shows little cross reactivity with other kinases. Therefore, these two compounds could not be expected as dual inhibitors for PIM1 and CK2. On the other hand, tryptanthrin is thought to have relatively high possibility to show dual inhibitory activity for PIM1 and CK2 compared to SGI-1776 and ETP-45299. Since tryptanthrin is small flat-form consisting of an indole ring and a quinazoline ring, it could be stabilized in the ATP-binding site of both kinases *via* maintenance of hydrophobic interactions with nearby nonpolar amino acids and formation of hydrogen bond with Lys67 of PIM1 and Lys68 of CK2, respectively, at the conserved active site. Further assessments for inhibition of CK2 activity will allow us to resolve whether tryptanthrin can act as a novel dual inhibitor. It is meaningful that tryptanthrin shows the possibility of functional duality since both PIM1 and CK2 are considered to be critical regulators for rendering radioresistance. Recent study has found that the inhibition of CK2 is correlated with radiosensitization *via* suppressing proliferative activity of Stat3 in NSCLC cells [56]. Blocking single radioresistant signaling used by a specific inhibitor might be, at least in part, insufficient for the regulation of radiosensitivity, because it could not be completely excluded the possibility that compensatory signaling response mediated by CK2 as a crosstalk pathway might be involved in radioresistance of NSCLC [60]. Therefore, using a dual inhibitor could be a promising strategy to enhance the efficacy of radiosensitization *via* blocking both radiation-associated responses at the same time.

Radiosensitizers have been developed in combination with radiotherapy to enhance therapeutic efficacy. Promising radiosensitizers are considered to have high tumor cell specificity to maximize effects of treatment and render few adverse effects such as normal cell damage. Traditional radiosensitizers including classic chemotherapeutic agents focused on tumor microenvironments such as high frequency of DNA replication and mitotic division and hypoxia, which showed poor specificity to cancer cells. Then, many research groups make a great effort to establish target-based radiosensitizing strategies for tumor selectivity and the availability of molecular markers. For example, inhibition of the EGFR by small molecule tyrosine kinase inhibitors, such as erlotinib, or monoclonal antibodies, such as cetuximab, has been shown to radiosensitize a limited number of NSCLC cell lines *in vitro* and *in vivo* [61–63]. In the same context, we found that PIM1 served as a potential pharmacological target for the radiosensitization of NSCLC cells because PIM1 as an upstream kinase in response to IR played a critical role in radioresistant NSCLC cells [7]. In addition, NSCLC cells underwent apoptotic death only by a combinational treatment with IR and PIM1 inhibitors compared to no cytotoxicity by inhibitors alone. It means that SGI-1776, ETP-45299 and tryptanthrin might be considered as pharmacologically promising radiosensitizers in a manner of safety. These PIM1 inhibitors sensitized NSCLC cells to radiation through specifically targeting PIM1-mediated signaling, and it could be also a useful strategy to apply them for treating other radioresistant cancer cells including pancreatic ductal adenocarcinoma cells and squamocellular carcinoma of head and neck, which of radioresistance are mediated by overexpressed PIM1 [25,64]. Our present study supports the evidence that understanding tumor-specific response to IR and investigating molecular mechanism of radioresistance in tumors would provide the basis for the identification of pharmacological targets for radiation susceptibility and then for the development of target-based radiosensitizers.

In summary, our study revealed radiosensitizing activity of SGI-1776, ETP-45299 and tryptanthrin, PIM1 specific inhibitors, in NSCLC cells and identified its mechanisms of action which include disruption of trimeric complexes between PRAS40, FOXO3a and 14-3-3, and then increased FOXO3a nuclear localization, which trigger transcription of pro-apoptotic genes, followed by apoptotic death. These PIM1 inhibitors have the potential to considerably increase the therapeutic index of radiation therapy. Therefore, our study provides the evidence for future development of SGI-1776, ETP-45299 and tryptanthrin as a novel class of radiosensitizing drugs against PIM1-positive NSCLC and, possibly, other types of human cancers.

Acknowledgements

This work was supported by Nuclear R&D Program (2012-0006383) and by Basic Science Research Program (2012-0003201) through the National Research Foundation of Korea funded by the Ministry of Education, Science and Technology.

References

[1] Bergqvist AS, Brattstrom D, Bergqvist M, Brodin O, Wagenius G, Zetterberg LA. The frequency of micronuclei in lung cancer cell lines and their correlation to intrinsic radiation sensitivity. Anticancer Research 2001;21:3853–6.
[2] Jemal A, Siegel R, Ward E, Murray T, Xu J, Smigal C, et al. Cancer Statistics, 2006. CA: A Cancer Journal for Clinicians 2006;56:106–30.
[3] Bradley JD, Paulus R, Graham MV, Ettinger DS, Johnstone DW, Pilepich MV, et al. Phase ii trial of postoperative adjuvant paclitaxel/carboplatin and thoracic radiotherapy in resected stage ii and iiia non-small-cell lung cancer: promising long-term results of the radiation therapy oncology group–rtog 9705. Journal of Clinical Oncology 2005;23:3480–7.
[4] Brognard J, Clark AS, Ni Y, Dennis PA. Akt/protein kinase b is constitutively active in non-small cell lung cancer cells and promotes cellular survival and resistance to chemotherapy and radiation. Cancer Research 2001;61:3986–97.
[5] Cao C, Mu Y, Hallahan DE, Lu B. Xiap and survivin as therapeutic targets for radiation sensitization in preclinical models of lung cancer. Oncogene 2004;23:7047–52.
[6] Dritschilo A, Huang CH, Rudin CM, Marshall J, Collins B, Dul JL, et al. Phase i study of liposome-encapsulated c-raf antisense oligodeoxyribonucleotide infusion in combination with radiation therapy in patients with advanced malignancies. Clinical Cancer Research 2006;12:1251–9.

[7] Kim W, Youn H, Seong KM, Yang HJ, Yun YJ, Kwon T, et al. Pim1-activated pras40 regulates radioresistance in non-small cell lung cancer cells through interplay with foxo3a, 14-3-3 and protein phosphatases. Radiation Research 2011;176:539–52.
[8] Nishimura Y, Nakagawa K, Takeda K, Tanaka M, Segawa Y, Tsujino K, et al. Phase i/ii trial of sequential chemoradiotherapy using a novel hypoxic cell radiosensitizer, doranidazole (pr-350), in patients with locally advanced non-small-cell lung cancer (wjtog-0002). International Journal of Radiation Oncology, Biology, Physics 2007;69:786–92.
[9] Hillman GG, Singh-Gupta V, Runyan L, Yunker CK, Rakowski JT, Sarkar FH, et al. Soy isoflavones radiosensitize lung cancer while mitigating normal tissue injury. Radiotherapy and Oncology 2011;101:329–36.
[10] Toschi L, Cappuzzo F. Impact of biomarkers on non-small cell lung cancer treatment. Targeted Oncology 2010;5:5–17.
[11] Wang Z, Bhattacharya N, Mixter PF, Wei W, Sedivy J, Magnuson NS. Phosphorylation of the cell cycle inhibitor p21cip1/waf1 by pim-1 kinase. Biochimica et Biophysica Acta 2002;1593:45–55.
[12] Dautry F, Weil D, Yu J, Dautry-Varsat A. Regulation of pim and myb mrna accumulation by interleukin 2 and interleukin 3 in murine hematopoietic cell lines. Journal of Biological Chemistry 1988;263:17615–20.
[13] Lilly M, Le T, Holland P, Hendrickson SL. Sustained expression of the pim-1 kinase is specifically induced in myeloid cells by cytokines whose receptors are structurally related. Oncogene 1992;7:727–32.
[14] van Lohuizen M, Verbeek S, Krimpenfort P, Domen J, Saris C, Radaszkiewicz T, et al. Predisposition to lymphomagenesis in pim-1 transgenic mice: cooperation with c-myc and n-myc in murine leukemia virus-induced tumors. Cell 1989;56:673–82.
[15] van Lohuizen M, Breuer M, Berns A. N-myc is frequently activated by proviral insertion in mulv-induced t cell lymphomas. EMBO Journal 1989;8:133–6.
[16] Breuer M, Slebos R, Verbeek S, van Lohuizen M, Wientjens E, Berns A. Very high frequency of lymphoma induction by a chemical carcinogen in pim-1 transgenic mice. Nature 1989;340:61–3.
[17] Breuer M, Wientjens E, Verbeek S, Slebos R, Berns A. Carcinogen-induced lymphomagenesis in pim-1 transgenic mice: dose dependence and involvement of myc and ras. Cancer Research 1991;51:958–63.
[18] van der Houven van Oordt CW, Schouten TG, van Krieken JH, van Dierendonck JH, van der Eb AJ, Breuer ML. X-ray-induced lymphomagenesis in e mu-pim-1 transgenic mice: an investigation of the co-operating molecular events. Carcinogenesis 1998;19:847–53.
[19] Bullock AN, Debreczeni J, Amos AL, Knapp S, Turk BE. Structure and substrate specificity of the pim-1 kinase. Journal of Biological Chemistry 2005;280:41675–82.
[20] Kumar A, Mandiyan V, Suzuki Y, Zhang C, Rice J, Tsai J, et al. Crystal structures of proto-oncogene kinase pim1: a target of aberrant somatic hypermutations in diffuse large cell lymphoma. Journal of Molecular Biology 2005;348:183–93.
[21] Jacobs MD, Black J, Futer O, Swenson L, Hare B, Fleming M, et al. Pim-1 ligand-bound structures reveal the mechanism of serine/threonine kinase inhibition by ly294002. Journal of Biological Chemistry 2005;280:13728–34.
[22] Qian KC, Wang L, Hickey ER, Studts J, Barringer K, Peng C, et al. Structural basis of constitutive activity and a unique nucleotide binding mode of human pim-1 kinase. Journal of Biological Chemistry 2005;280:6130–7.
[23] Aho TL, Sandholm J, Peltola KJ, Mankonen HP, Lilly M, Koskinen PJ. Pim-1 kinase promotes inactivation of the pro-apoptotic bad protein by phosphorylating it on the ser112 gatekeeper site. FEBS Letters 2004;571:43–9.
[24] Gu JJ, Wang Z, Reeves R, Magnuson NS. Pim1 phosphorylates and negatively regulates ask1-mediated apoptosis. Oncogene 2009;28:4261–71.
[25] Peltola K, Hollmen M, Maula SM, Rainio E, Ristamaki R, Luukkaa M, et al. Pim-1 kinase expression predicts radiation response in squamocellular carcinoma of head and neck and is under the control of epidermal growth factor receptor. Neoplasia 2009;11:629–36.
[26] Chen DJ, Nirodi CS. The epidermal growth factor receptor: a role in repair of radiation-induced DNA damage. Clinical Cancer Research 2007;13:6555–60.
[27] Cheney IW, Yan S, Appleby T, Walker H, Vo T, Yao N, et al. Identification and structure–activity relationships of substituted pyridones as inhibitors of pim-1 kinase. Bioorganic and Medicinal Chemistry Letters 2007;17:1679–83.
[28] Debreczeni JE, Bullock AN, Atilla GE, Williams DS, Bregman H, Knapp S, et al. Ruthenium half-sandwich complexes bound to protein kinase pim-1. Angewandte Chemie International Ed In English 2006;45:1580–5.
[29] Pogacic V, Bullock AN, Fedorov O, Filippakopoulos P, Gasser C, Biondi A, et al. Structural analysis identifies imidazo[1,2-b]pyridazines as pim kinase inhibitors with in vitro antileukemic activity. Cancer Research 2007;67:6916–24.
[30] Morwick T. Pim kinase inhibitors: a survey of the patent literature. Expert Opinion on Therapeutic Patents 2010;20:193–212.
[31] Zhang Y, Wang Z, Li X, Magnuson NS. Pim kinase-dependent inhibition of c-myc degradation. Oncogene 2008;27:4809–19.
[32] Kim W, Yang HJ, Youn H, Yun YJ, Seong KM, Youn B. Myricetin inhibits akt survival signaling and induces bad-mediated apoptosis in a low dose ultraviolet (uv)-b-irradiated hacat human immortalized keratinocytes. Journal of Radiation Research 2010;51:285–96.
[33] Valerie K, Yacoub A, Hagan MP, Curiel DT, Fisher PB, Grant S, et al. Radiation-induced cell signaling: inside-out and outside-in. Molecular Cancer Therapeutics 2007;6:789–801.
[34] Nascimento EB, Ouwens DM. Pras40: target or modulator of mtorc1 signalling and insulin action? Archives of Physiology and Biochemistry 2009;115:163–75.
[35] Shimaya A, Kovacina KS, Roth RA. On the mechanism for neomycin reversal of wortmannin inhibition of insulin stimulation of glucose uptake. Journal of Biological Chemistry 2004;279:55277–82.
[36] Brunet A, Bonni A, Zigmond MJ, Lin MZ, Juo P, Hu LS, et al. Akt promotes cell survival by phosphorylating and inhibiting a forkhead transcription factor. Cell 1999;96:857–68.
[37] Brunet A, Kanai F, Stehn J, Xu J, Sarbassova D, Frangioni JV, et al. 14-3-3 transits to the nucleus and participates in dynamic nucleocytoplasmic transport. Journal of Cell Biology 2002;156:817–28.
[38] Kim KW, Mutter RW, Cao C, Albert JM, Freeman M, Hallahan DE, et al. Autophagy for cancer therapy through inhibition of pro-apoptotic proteins and mammalian target of rapamycin signaling. Journal of Biological Chemistry 2006;281:36883–90.
[39] Qiu W, Carson-Walter EB, Liu H, Epperly M, Greenberger JS, Zambetti GP, et al. Puma regulates intestinal progenitor cell radiosensitivity and gastrointestinal syndrome. Cell Stem Cell 2008;2:576–83.
[40] Zanella F, Link W, Carnero A. Understanding foxo, new views on old transcription factors. Current Cancer Drug Targets 2010;10:135–46.
[41] Mumenthaler SM, Ng PY, Hodge A, Bearss D, Berk G, Kanekal S, et al. Pharmacologic inhibition of pim kinases alters prostate cancer cell growth and resensitizes chemoresistant cells to taxanes. Molecular Cancer Therapeutics 2009;8:2882–93.
[42] Chen LS, Redkar S, Bearss D, Wierda WG, Gandhi V. Pim kinase inhibitor, sgi-1776, induces apoptosis in chronic lymphocytic leukemia cells. Blood 2009;114:4150–7.
[43] Swords R, Kelly K, Carew J, Nawrocki S, Mahalingam D, Sarantopoulos J, et al. The pim kinases: new targets for drug development. Current Drug Targets 2011;12:2059–66.
[44] Blanco-Aparicio C, Collazo AM, Oyarzabal J, Leal JF, Albaran MI, Lima FR, et al. Pim 1 kinase inhibitor etp-45299 suppresses cellular proliferation and synergizes with pi3k inhibition. Cancer Letters 2011;300:145–53.
[45] Chen LS, Redkar S, Taverna P, Cortes JE, Gandhi V. Mechanisms of cytotoxicity to pim kinase inhibitor, sgi-1776, in acute myeloid leukemia. Blood 2011;118:693–702.
[46] Ishihara T, Kohno K, Ushio S, Iwaki K, Ikeda M, Kurimoto M. Tryptanthrin inhibits nitric oxide and prostaglandin e(2) synthesis by murine macrophages. European Journal of Pharmacology 2000;407:197–204.
[47] Recio MC, Cerda-Nicolas M, Potterat O, Hamburger M, Rios JL. Anti-inflammatory and antiallergic activity in vivo of lipophilic isatis tinctoria extracts and tryptanthrin. Planta Medica 2006;72:539–46.
[48] Yu ST, Chen TM, Tseng SY, Chen YH. Tryptanthrin inhibits mdr1 and reverses doxorubicin resistance in breast cancer cells. Biochemical and Biophysical Research Communications 2007;358:79–84.
[49] Merkel AL, Meggers E, Ocker M. Pim1 kinase as a target for cancer therapy. Expert Opinion on Investigational Drugs 2012;21:425–36.
[50] Bullock AN, Debreczeni JE, Fedorov OY, Nelson A, Marsden BD, Knapp S. Structural basis of inhibitor specificity of the human protooncogene proviral insertion site in moloney murine leukemia virus (pim-1) kinase. Journal of Medicinal Chemistry 2005;48:7604–14.
[51] Qian K, Wang L, Cywin CL, Farmer 2nd BT, Hickey E, Homon C, et al. Hit to lead account of the discovery of a new class of inhibitors of pim kinases and crystallographic studies revealing an unusual kinase binding mode. Journal of Medicinal Chemistry 2009;52:1814–27.
[52] Tsuhako AL, Brown DS, Koltun ES, Aay N, Arcalas A, Chan V, et al. The design, synthesis, and biological evaluation of pim kinase inhibitors. Bioorganic and Medicinal Chemistry Letters 2012;22:3732–8.
[53] Lopez-Ramos M, Prudent R, Moucadel V, Sautel CF, Barette C, Lafanechere L, et al. New potent dual inhibitors of ck2 and pim kinases: discovery and structural insights. FASEB Journal 2010;24:3171–85.
[54] Litchfield DW. Protein kinase ck2: structure, regulation and role in cellular decisions of life and death. Biochemical Journal 2003;369:1–15.
[55] Piazza F, Manni S, Ruzzene M, Pinna LA, Gurrieri C, Semenzato G. Protein kinase ck2 in hematologic malignancies: reliance on a pivotal cell survival regulator by oncogenic signaling pathways. Leukemia 2012;26:1174–9.
[56] Lin YC, Hung MS, Lin CK, Li JM, Lee KD, Li YC, et al. Ck2 inhibitors enhance the radiosensitivity of human non-small cell lung cancer cells through inhibition of stat3 activation. Cancer Biotherapy and Radiopharmaceuticals 2011;26:381–8.
[57] Pierre F, Stefan E, Nedellec AS, Chevrel MC, Regan CF, Siddiqui-Jain A, et al. 7-(4h-1,2,4-Triazol-3-yl)benzo[c][2,6]naphthyridines: a novel class of pim kinase inhibitors with potent cell antiproliferative activity. Bioorganic and Medicinal Chemistry Letters 2011;21:6687–92.
[58] Pierre F, Regan CF, Chevrel MC, Siddiqui-Jain A, Macalino D, Streiner N, et al. Novel potent dual inhibitors of ck2 and pim kinases with antiproliferative activity against cancer cells. Bioorganic and Medicinal Chemistry Letters 2012;22:3327–31.
[59] Pagano MA, Bain J, Kazimierczuk Z, Sarno S, Ruzzene M, Di Maira G, et al. The selectivity of inhibitors of protein kinase ck2: an update. Biochemical Journal 2008;415:353–65.
[60] Drygin D, Haddach M, Pierre F, Ryckman DM. Potential use of selective and nonselective pim kinase inhibitors for cancer therapy. Journal of Medicinal Chemistry 2012;55:8199–208.

[61] Bianco C, Tortora G, Bianco R, Caputo R, Veneziani BM, Damiano V, et al. Enhancement of antitumor activity of ionizing radiation by combined treatment with the selective epidermal growth factor receptor-tyrosine kinase inhibitor zd1839 (iressa). Clinical Cancer Research 2002;8:3250–8.
[62] Chinnaiyan P, Huang S, Vallabhaneni G, Armstrong E, Varambally S, Tomlins SA, et al. Mechanisms of enhanced radiation response following epidermal growth factor receptor signaling inhibition by erlotinib (tarceva). Cancer Research 2005;65:3328–35.
[63] Wang M, Morsbach F, Sander D, Gheorghiu L, Nanda A, Benes C, et al. Egf receptor inhibition radiosensitizes nsclc cells by inducing senescence in cells sustaining DNA double-strand breaks. Cancer Research 2011;71: 6261–9.
[64] Xu D, Allsop SA, Witherspoon SM, Snider JL, Yeh JJ, Fiordalisi JJ, et al. The oncogenic kinase pim-1 is modulated by k-ras signaling and mediates transformed growth and radioresistance in human pancreatic ductal adenocarcinoma cells. Carcinogenesis 2011;32:488–95.